

1999

Diffusion and Localization of Ultra-Cold Particles on Rough Substrates

A. Stepaniants

D. Sarkisov

See next page for additional authors

Follow this and additional works at: http://digitalcommons.uri.edu/phys_facpubs

Terms of Use

All rights reserved under copyright.

Citation/Publisher Attribution

A.Stepaniants, D.Sarkisov, and A.E. Meyerovich. Diffusion and Localization of Ultra-Cold Particles on Rough Substrates *J.Low Temp.Phys.*,114, 371 (1999).

Available at: <http://dx.doi.org/10.1023/A:1022584518699>

This Article is brought to you for free and open access by the Physics at DigitalCommons@URI. It has been accepted for inclusion in Physics Faculty Publications by an authorized administrator of DigitalCommons@URI. For more information, please contact digitalcommons@etal.uri.edu.

Authors

A. Stepaniants, D. Sarkisov, and A. E. Meyerovich

Diffusion and localization of ultra-cold particles on rough substrates

A. Stepaniants, D. Sarkisov, and A. Meyerovich

Department of Physics, University of Rhode Island,

Kingston, RI 02881

(September 28, 1998)

Abstract

Diffusion and localization of ultra-cold particles moving along randomly corrugated substrates is analyzed quasianalytically. The particles are either bound to the substrate or pressed to it by the external holding field. The localization length and diffusion coefficient are expressed explicitly via the correlation radius of surface inhomogeneities. This quantum bouncing ball problem with a random rough wall is solved analytically in three limiting cases of longwave particles, large gaps between bound states, and single-state occupancy. Elsewhere, the diffusion coefficient and localization length are evaluated numerically for Gaussian correlation of inhomogeneities. The results are applied to ultra-cold neutrons in the gravitational trap, electrons on helium and hydrogen surfaces, and hydrogen particles bound to helium surface. Experimental observation of weak $2D$ localization for neutrons and electrons requires further cooling and substrate preparation.

PACS: 61.12.-q, 73.20.Fz, 67.90.+z

I. INTRODUCTION

Elastic scattering of $2D$ particles by any random inhomogeneities, including the boundary ones, results in localization [1–8]. This should be true for particles that are bound to or adsorbed on a randomly corrugated substrate. If the size of the bound state is relatively large and the particles can move along the substrate, the particle mean free path, diffusion coefficient, and localization length are determined by the scattering by substrate inhomogeneities. Sometimes, the inhomogeneity of the boundary is easily translated into an inhomogeneous $2D$ potential $W(\mathbf{s})$, and one deals with a standard $2D$ diffusion or localization problem. Often, the problem is somewhat different. For example, instead of a random potential problem one can encounter a problem with a random boundary condition, *e.g.*, the problem of particles with the boundary condition $\Psi = 0$ on a wall $x = \xi(y, z) \equiv \xi(\mathbf{s})$ with random inhomogeneities $\xi(\mathbf{s})$, $\langle \xi \rangle = 0$. Though it is clear that this problem is almost the same as the problem with the random $2D$ bulk potential $W(y, z)$, the explicit expressions for the localization parameters via the wall profile are unknown. This is especially important in the weak localization limit with an exponentially large localization length for which even a relatively small uncertainty in the index may lead to a difference by several orders of magnitude. Another feature of this problem is that the correlation radius R of surface inhomogeneities can be large while the analog of this parameter for scattering by bulk impurities, namely, the range of the scattering potential $W(\mathbf{s})$, is usually small.

Below we express diffusion and localization parameters of adsorbed particles directly via the wall profile. Recently we developed a simple formalism [9,10] that allows an exact mapping of the transport problems for systems with random boundaries onto problems with perfect boundaries and randomly distorted bulk. The approach is based on an explicit Migdal-like coordinate transformation that flattens the boundary and, in the process, distorts the bulk. In what follows, we apply a similar formalism to particles bound to and moving along the randomly corrugated wall or substrate.

Generically, the problem can be described as a quantum bouncing ball problem with

a static random rough wall $x = \xi(\mathbf{s})$ with an average position $\langle x \rangle_\xi = \langle \xi(\mathbf{s}) \rangle = 0$. We consider particles $\epsilon = p^2/2m$ that are either pressed to the inhomogeneous wall by the external holding potential $U(x)$, $U(x \rightarrow \infty) \rightarrow \infty$ (this can be the gravitational, electric, or magnetic field), or are bound to the wall by some attractive wall-induced potential $U(x) < 0$, $U(x \rightarrow \infty) \rightarrow 0$. In both cases, the structure of the potential ensures the discrete energy spectrum ϵ_j of finite motion in x direction and continuous free motion along the wall with the wave vector \mathbf{q} , $\epsilon_{j\mathbf{q}} = \epsilon_j + q^2/2m$. This formulation is typical for ultra-cold neutrons bouncing from the trap walls in the gravitational field [11], electrons on the helium or hydrogen surface in electric field, adsorbed particles with a relatively large size of the bound state, *etc.* The results for all these various systems are almost identical. Some modifications are required to adjust the results to particles in films with two inhomogeneous walls so that to account for interference caused by interwall correlations [10].

As usual for weak localization processes, we start from the diffusion problem and apply the expressions for the diffusion coefficient D and mean free path \mathcal{L} to the weak localization problem. In our case, the localization length \mathcal{R} for particles with energy E is (*cf.* Refs. [1,3])

$$\mathcal{R}(E) = \mathcal{L}(E) \exp[\pi m S(E) D(E)] \quad (1)$$

where S is the number of minibands $\epsilon_{j\mathbf{q}}$ accessible for a particle with energy E .

There are several experimentally feasible types of correlation functions of surface inhomogeneities [13,14]. In analytical calculations we do not need to specify this correlator,

$$\begin{aligned} \zeta(|\mathbf{s}|) &= \langle \xi(\mathbf{s}_1) \xi(\mathbf{s}_1 + \mathbf{s}) \rangle \equiv \int \xi(\mathbf{s}_1) \xi(\mathbf{s}_1 + \mathbf{s}) d\mathbf{s}_1, \\ \zeta(\mathbf{q}) &= \int d^2s e^{i\mathbf{q}\cdot\mathbf{s}/\hbar} \zeta(\mathbf{s}) = \xi(\mathbf{q}) \xi(-\mathbf{q}) \end{aligned} \quad (2)$$

In numerical applications, we assume that the correlation function is Gaussian,

$$\zeta(\mathbf{s}) = \ell^2 \exp\left(-s^2/2R^2\right), \quad \zeta(\mathbf{q}) = 2\pi\ell^2 R^2 \exp\left(-q^2 R^2/2\right). \quad (3)$$

II. TRANSPORT EQUATION

The coordinate transformation

$$X = x - \xi(\mathbf{s}), \quad Y = y, \quad Z = z \quad (4)$$

makes the wall $x = \xi(\mathbf{s})$ in the new coordinate system flat, $X = 0$. In new coordinate and momentum variables that are canonically conjugate to (4),

$$\hat{p}_x = \hat{P}_x, \quad \hat{p}_{y,z} = \hat{P}_{y,z} - \xi'_{y,z} \hat{P}_x, \quad (5)$$

the Hamiltonian $\widehat{H}_0(\hat{\mathbf{p}}, x) = \hat{p}^2/2m + U(x)$ acquires the random inhomogeneous part \widehat{V} ,

$$\begin{aligned} \widehat{H}_0(\hat{\mathbf{p}}, x) &= \widehat{H}_0(\hat{\mathbf{P}}, X) + \widehat{V} = \frac{\hat{P}^2}{2m} + U(X) + \widehat{V}, \\ \widehat{V} &= \frac{\partial U}{\partial X} \xi(\mathbf{s}) - \frac{1}{2m} \hat{P}_x \left[\hat{\mathbf{P}}_s \frac{\partial \xi(\mathbf{s})}{\partial \mathbf{s}} + \frac{\partial \xi(\mathbf{s})}{\partial \mathbf{s}} \hat{\mathbf{P}}_s \right]. \end{aligned} \quad (6)$$

To illustrate the method and simplify the equations, we will start from the particles in the linear (gravitational or electric) holding potential $U(x) = mgx$. Then the problem is best described by five parameters with the dimensionality of length: the characteristic height and radius of surface inhomogeneities ℓ and R , spatial scale of the (first) bound state $L = (2m^2g)^{-1/3}$, particle wavelength λ , and the amplitude of particle jumps H in the field mg , $H \sim L^3/\lambda^2$. The first two parameters describe the wall, the third characterizes the field, and the last two - the particle energy $E = mgH$. The perturbative approach to the Hamiltonian (6) requires that $\ell \ll R, H$. This is the main restriction on the results below. The quantum effects in scattering are characterized by parameters R/λ and the importance of quantization of spectrum - by the number S of occupied or accessible minibands $\epsilon_{j\mathbf{q}}$, $S \sim (H/L)^{3/2}$. We will present the results for both quantum and quasiclassical regimes. Though one cannot expect localization in the quasiclassical regime $H \gg L$, the transport calculations for a quasiclassical bouncing ball are still worth doing.

The unperturbed wave functions for the Hamiltonian \widehat{H}_0 with the flat wall are the Airy functions

$$\Psi_{j\mathbf{q}}(x, \mathbf{s}) = e^{i\mathbf{q}\mathbf{s}} A_j \Phi \left((2m^2g)^{1/3} \left(x - \frac{\epsilon_j}{mg} \right) \right) \quad (7)$$

where A_j are the normalization coefficients, and the energy eigenvalues ϵ_j are given by the zeroes of the Airy function, $\Phi(-\epsilon_j/mgL) = 0$. The matrix elements of the perturbation \widehat{V} are

$$V_{jj'}(\mathbf{q}, \mathbf{q}') = \xi(\mathbf{q}' - \mathbf{q}) \left(mg\delta_{jj'} + \frac{1}{2m}(q'^2 - q^2)A_j A_{j'} M_{jj'} \right), \quad (8)$$

$$M_{jj'} = \int_0^\infty \Phi \left((2m^2g)^{1/3} \left(x - \frac{\epsilon_j}{mg} \right) \right) \frac{d}{dx} \Phi \left((2m^2g)^{1/3} \left(x - \frac{\epsilon_{j'}}{mg} \right) \right) dx$$

The transition probabilities in the collision integral $W_{jj'}(\mathbf{q}, \mathbf{q}')$ are determined by the squares of the matrix elements $V_{jj'}(\mathbf{q}, \mathbf{q}')$ (8) and, after averaging over the wall inhomogeneities ξ , are expressed via the correlation function $\zeta(\mathbf{q}' - \mathbf{q})$ as

$$W_{jj'}(\mathbf{q}, \mathbf{q}') = \left\langle |V_{jj'}(\mathbf{q}, \mathbf{q}')|^2 \right\rangle_\xi = \zeta(\mathbf{q}' - \mathbf{q}) \left(m^2 g^2 \delta_{jj'} + \frac{1}{4m^2} (q'^2 - q^2)^2 A_j^2 A_{j'}^2 M_{jj'}^2 \right). \quad (9)$$

These transition probabilities include both the intraband scattering and interband transitions.

It is possible to show (see Appendix and Ref. [12]) that the term in brackets in Eq.(9) in combination with the energy δ -functions $\delta(\epsilon_{j\mathbf{q}} - \epsilon_{j'\mathbf{q}'})$, *i.e.*, for the states with $\epsilon_{j\mathbf{q}} = \epsilon_{j'\mathbf{q}'}$, is equal to $m^2 g^2$. This simplification is not accidental. It turns out that for a wide class of *transport* problems the only important information concerning the holding potential $U(x)$ is the spectrum of the bound states $\epsilon_{j\mathbf{q}}$. If one is interested only in the states with $\epsilon_{j\mathbf{q}} = \epsilon_{j'\mathbf{q}'}$, all other details of the holding potential $U(x)$ disappear from the expressions for $W_{jj'}(\mathbf{q}, \mathbf{q}')$ which obtain the general form (see Eq.(45) from the Appendix)

$$W_{jj'}(\mathbf{q}, \mathbf{q}') \delta(\epsilon_{j\mathbf{q}} - \epsilon_{j'\mathbf{q}'}) = \frac{1}{4m^2} \zeta(\mathbf{q}' - \mathbf{q}) \left| \frac{d\Psi_j(0)}{dX} \right|^2 \left| \frac{d\Psi_{j'}(0)}{dX} \right|^2 \delta(\epsilon_{j\mathbf{q}} - \epsilon_{j'\mathbf{q}'}). \quad (10)$$

where $\Psi_j(X)$ are the eigenfunctions of the "unperturbed" Hamiltonian $\widehat{H}_0(\widehat{\mathbf{P}}, X)$ (6) with the flat wall. In the case of the potential $U = mgX$, $\Psi_j(X)$ are the Airy functions (7) and the transition probabilities (9),(10) are given by Eq.(46) of the Appendix:

$$W_{jj'}(\mathbf{q}, \mathbf{q}') \delta(\epsilon_{j\mathbf{q}} - \epsilon_{j'\mathbf{q}'}) = m^2 g^2 \zeta(\mathbf{q}' - \mathbf{q}) \delta(\epsilon_{j\mathbf{q}} - \epsilon_{j'\mathbf{q}'}). \quad (11)$$

Since the general expression for the collision operator in the transport equation,

$$\frac{dn_j}{dt} = 2\pi \sum_{j'=1}^S \int \frac{d^2q'}{(2\pi)^2} W_{jj'}(\mathbf{q}, \mathbf{q}') \delta(\epsilon_{j\mathbf{q}} - \epsilon_{j'\mathbf{q}'} [n_{j'} - n_j], \quad (12)$$

contains such energy δ -functions in the integrand, the collision operator is determined only by the profile of wall inhomogeneities $\zeta(\mathbf{q}' - \mathbf{q})$, particle spectrum $\epsilon_{j\mathbf{q}}$, and the derivatives of the unperturbed wave functions on the wall ($n_j(\mathbf{q})$ is the distribution function for particles in the miniband $\epsilon_{j\mathbf{q}}$). This equation can be used for a wide class of transport problems with particles that are bound to the randomly corrugated wall by an arbitrary potential $U(x)$.

Density gradient $\nabla n_j^{(0)}(\mathbf{q})$ causes particle diffusion along the surface for the particles in each miniband $\epsilon_{j\mathbf{q}}$. Then the transport equation (12) for particles in the linear holding potential $U = mgx$ becomes a set of integral equations coupled via transitions probabilities (11) $W_{jj'} = m^2 g^2 \zeta(\mathbf{q}' - \mathbf{q})$ in the collision operator:

$$\frac{\mathbf{q}}{m} \cdot \nabla n_j^{(0)}(\mathbf{q}) = 2\pi m^2 g^2 \sum_{j'} \int \frac{d\mathbf{q}}{(2\pi)^2} \zeta(\mathbf{q}' - \mathbf{q}) (\delta n_{j'\mathbf{q}'} - \delta n_{j\mathbf{q}}) \delta(\epsilon_{j\mathbf{q}} - \epsilon_{j'\mathbf{q}'}). \quad (13)$$

For a single particle with the energy E , the summation in (13) takes place over all S minibands $\epsilon_{j\mathbf{q}}$ that are accessible to a particle with energy E , *i.e.*, for all the values of j' for which $\epsilon_{j'}(q=0) \leq E$. The particle has the same probability to be in any accessible miniband, and we have to follow the diffusion spread of the narrow wave packets $n_{j\mathbf{q}}^{(0)} = n^{(0)}(\epsilon_{j\mathbf{q}})$ centered around the energy $\epsilon_{j\mathbf{q}} = E$:

$$\begin{aligned} n_{j\mathbf{q}} &= n_{j\mathbf{q}}^{(0)} + \delta n_{j\mathbf{q}}, \\ \delta n_{j\mathbf{q}} &= \chi_j(\mathbf{q}) \mathbf{q} \cdot \nabla n_j^{(0)}(\mathbf{q}) / m \end{aligned} \quad (14)$$

The transport equation (13) reduces to

$$q_j \cos \theta = m^3 g^2 \sum_{j'} \int \frac{d\theta'}{2\pi} \zeta(q_j, q_{j'}, \theta - \theta') (q_{j'} \cos \theta' \chi_{j'}(\theta') - q_j \cos \theta \chi_j(\theta)) \quad (15)$$

We look for a solution in the form of angular harmonics

$$\chi_j(\theta) = \frac{1}{2} \chi_j^{(0)} + \sum_{s=1}^{\infty} \chi_j^{(s)} \cos(s\theta), \quad W(\theta) = \frac{1}{2} W^{(0)} + \sum_{s=1}^{\infty} W^{(s)} \cos(s\theta) \quad (16)$$

The diffusion current is determined by the zeroth harmonic of the distribution χ :

$$\vec{J} = \frac{1}{2m^2} \vec{\nabla} \rho \frac{1}{S} \sum_j q_j^2 \chi_j^{(0)} \quad (17)$$

In the dimensionless variables

$$\begin{aligned} \alpha &= \sqrt{2mER} = \left(HR^2/L^3 \right)^{1/2}, \quad \beta = R/L = R(2m^2g)^{1/3}, \\ \kappa_j &= \pi m^3 g^2 \ell^2 R^2 \chi_j^{(0)} / 2, \quad \tilde{\epsilon}_j = \epsilon_j / mgL, \quad z_j = q_j R = \sqrt{\alpha^2 - \beta^2 \tilde{\epsilon}_j}, \\ \widetilde{W}_{jj'} &= W_{jj'}(q_j, q_{j'}, \theta - \theta') / m^2 g^2 2\pi \ell^2 R^2 = \zeta(q_j, q_{j'}, \theta - \theta') / 2\pi \ell^2 R^2, \end{aligned} \quad (18)$$

the transport equation for this harmonic of the distribution has the form

$$z_j = \sum_{j'} \kappa_j \left(\widetilde{W}_{jj'}^{(1)} z_{j'} - \delta_{jj'} z_j \sum_k \widetilde{W}_{jk}^{(0)} \right). \quad (19)$$

The diffusion coefficient is equal to

$$D = -\frac{4R^2}{\pi m \beta^6 \ell^2 S} \sum_j z_j^2 \kappa_j, \quad (20)$$

and the mean free path $\mathcal{L} = 2D/v$ can be parameterized as

$$\mathcal{L} = 2mRD/\alpha \quad (21)$$

The information on D and the mean free path \mathcal{L} allows simple calculation of the $2D$ localization length \mathcal{R} [1,3]

$$\mathcal{R} = \mathcal{L} \exp \varphi(\alpha, \beta, \ell/R), \quad \varphi \equiv \pi m S D \quad (22)$$

(the dependence on ℓ is trivial since, according to Eq.(20), $D \propto R^2/\ell^2$ and ℓ does not enter Eqs.(19) for κ_j).

The dimensionless transition probability \widetilde{W} (11), (18) for the Gaussian correlations (3) is

$$\begin{aligned} \widetilde{W}_{jj'} &= \exp \left[-(z_j^2 + z_{j'}^2 - 2z_j z_{j'} \cos(\theta - \theta')) / 2 \right], \\ \widetilde{W}_{jj'}^{(0,1)} &= \left[{}_1F_1 \left(\frac{1}{2}; 2; -2z_j z_{j'} \right) \pm {}_1F_1 \left(\frac{3}{2}; 2; -2z_j z_{j'} \right) \right] \exp \left[-\frac{1}{2} (z_j - z_{j'})^2 \right]. \end{aligned} \quad (23)$$

III. DIFFUSION COEFFICIENT AND LOCALIZATION LENGTH

The transport equation (19) can be solved analytically in three limiting cases, namely, in the cases of the single-band occupancy, long-wave particles, and large spacing between bands. In the first case, the set of equations (19) reduces to a single linear equations. The second case corresponds to the quantum reflection when the main term in the scattering amplitude corresponds to $q \rightarrow 0$. In the third case, the separation between the bands is so large that the interband transitions are suppressed in comparison to intraband scattering and Eqs.(19) decouple from each other. Elsewhere, Eqs.(19) should be solved numerically.

In the first limiting case, only one (first) miniband is occupied, $S = 1$, and the transport equation (19) becomes trivial:

$$\begin{aligned} \varphi = \pi m D &= \frac{8\pi L^6}{R^2} \frac{\alpha^2 - 2.34\beta^2}{\zeta^{(0)}(q_1) - \zeta^{(1)}(q_1)} \\ &\rightarrow \frac{2R^2}{\beta^6 \ell^2} \frac{\alpha^2 - 2.34\beta^2}{{}_1F_1\left(\frac{3}{2}; 2; -2(\alpha^2 - 2.34\beta^2)\right)}. \end{aligned} \quad (24)$$

where φ is the localization exponent (22) and the last expression describes Gaussian correlations (3),(23). All particles are in the first miniband only if $1.53 < \alpha/\beta = qL < 2.02$ (at larger q the second miniband becomes accessible). In this case the localization is observable for $\beta = R/L \gtrsim (R/\ell)^{1/3}$. Together with the perturbation condition $\ell < L, R$ (in this case $H \sim L$), this restriction requires $\ell/L \lesssim L/R$.

The limiting case of the long-wave particles, $\alpha = R/\lambda \ll 1$, corresponds to quantum reflection. In this case, all the scattering probabilities are constants with the first harmonic equal to zero:

$$\widetilde{W}_{jj'}^{(1)} = 0, \quad \widetilde{W}_{jj'}^{(0)} = 2m^2 g^2 \zeta(\mathbf{q}=0), \quad (25)$$

and the solution of Eq.(19) yields

$$D(\alpha \ll 1, \beta) = \frac{2}{m^4 g^2 S^2 \zeta(0)} \sum_{j=1}^S (E - \epsilon_j) \rightarrow \frac{8}{5} \frac{HL^3}{mS\zeta(0)} \quad (26)$$

or, for Gaussian correlations,

$$D(\alpha \ll 1, \beta) = \frac{1}{\pi m^4 g^2 S^2 R^2 \ell^2} \sum_{j=1}^S (E - \epsilon_j) \rightarrow \frac{4}{5} \frac{HL^3}{\pi m S R^2 \ell^2} \quad (27)$$

(the last equations (26),(27) correspond to the quasiclassical limit of large $S \gg 1$; $E = mgH$).

In the third limiting case of large interband spacings $L^2/R\lambda \sim \alpha/\beta^2 \ll 1$ the interband transitions are suppressed and the transport equations (19) decouple. Then the diffusion coefficient is

$$D(\alpha/\beta^2 \ll 1) = \frac{4}{m^4 g^2 S} \sum_{j=1}^S \frac{E - \epsilon_j}{\zeta^{(0)}(2q_j \sin \frac{\theta}{2}) - \zeta^{(1)}(2q_j \sin \frac{\theta}{2})} \quad (28)$$

In the case of Gaussian correlations

$$\zeta_j^{(0)} - \zeta_j^{(1)} = 4\pi R^2 \ell^2 {}_1F_1(3/2; 2; -2(\alpha^2 - \beta^2 \tilde{\epsilon}_j)), \quad (29)$$

and the diffusion coefficient is

$$D(\alpha/\beta^2 \ll 1) = \frac{1}{\pi m^4 g^2 R^2 \ell^2 S} \sum_{j=1}^S \frac{E - \epsilon_j}{{}_1F_1(3/2; 2; -2(\alpha^2 - \beta^2 \tilde{\epsilon}_j))} \rightarrow \frac{5RH^4}{16\sqrt{2\pi}mL^3\ell^2S} \quad (30)$$

(the last equation is, again, quasiclassical).

In all other situations the transport equation can easily be solved numerically.

Let us also give the quasiclassical version of the transport equation (19). In the quasiclassical limit of large values of j , S , $\alpha^2/\beta^3 \gg 1$ (the last condition means that the transition probabilities are slow functions of j thus allowing to replace summation over levels by the integration), the explicit expressions for the energy levels ϵ_j can be obtained from the quasiclassical quantization condition:

$$\tilde{\epsilon}_j = \left[\frac{3\pi}{2} \left(j + \frac{1}{2} \right) \right]^{2/3}. \quad (31)$$

Then the number of accessible states S is

$$S = \frac{2}{3\pi} \left(\frac{\alpha}{\beta} \right)^3 \gg 1 \quad (32)$$

The quasiclassical transport equation in continuous variables

$$\sqrt{\alpha^2 - \beta^2 \tilde{\epsilon}_j} \rightarrow t, \quad \kappa_j \rightarrow \kappa(t) \quad (33)$$

has the form

$$\begin{aligned} \frac{\pi\beta^3}{2}t &= \int_0^\alpha \kappa(t') e^{-(t'-t)^2/2} \left[{}_1F_1\left(\frac{1}{2}; 2; -2tt'\right) - {}_1F_1\left(\frac{3}{2}; 2; -2tt'\right) \right] \sqrt{\alpha^2 - t'^2} dt' \\ &\quad - \kappa(t) t \int_0^\alpha e^{-(t'-t)^2/2} \left[{}_1F_1\left(\frac{1}{2}; 2; -2tt'\right) + {}_1F_1\left(\frac{3}{2}; 2; -2tt'\right) \right] \sqrt{\alpha^2 - t'^2} dt', \end{aligned} \quad (34)$$

while the diffusion coefficient is

$$D = -\frac{12}{\pi m \alpha^3 \beta^6} \frac{R^2}{\ell^2} \int_0^\alpha \kappa(t) \sqrt{\alpha^2 - t^2} t^3 dt \quad (35)$$

Instead of presenting separate numerical illustrations for localization and diffusion parameters, we will present the data for the exponent φ (22) that determines both the localization length and diffusion (or mobility) coefficient.

To have reasonable localization lengths, the exponent φ in Eq.(22) should not be very large, $\varphi \leq 20$. Since the above equations rely on the perturbation theory in amplitude and aperture of roughness, the parameter ℓ/R in the exponent φ cannot exceed 1. The exponent φ grows very rapidly with growing $\alpha = \sqrt{2mER} = (HR^2/L^3)^{1/2}$ and decreases with increasing $\beta = R(2m^2g)^{1/3} = R/L$. Therefore, in order to be able to observe localization, one should try to decrease the particle energy E , decrease the correlation radius R , increase the amplitude of inhomogeneities ℓ , and increase the pressing force mg . This means that for $\beta = R/L < H/L$ the minimal localization length corresponds to $\ell \sim R < H$, while for $\beta > H/L$ (a less probable physical scenario) one should consider $\ell \sim H < R$. Note, that relatively small values of φ often correspond to the range of α in which $\alpha/\beta^2 \ll 1$ and Eq.(30) yields

$$\varphi(\alpha/\beta^2 \ll 1) = \frac{1}{m^3 g^2 R^2 \ell^2} \sum_{j=1}^S \frac{E - \epsilon_j}{{}_1F_1\left[\frac{3}{2}; 2; -2(\alpha^2 - \beta^2 \tilde{\epsilon}_j)\right]} \rightarrow \frac{5\sqrt{\pi/2} H^4 R}{16\ell^2 L^3} \quad (36)$$

This equation shows that the localization length is the most sensitive to the particle velocity $v^2 = 2gH$ and the holding potential. The easiest way to estimate the numerical values of the diffusion coefficient D and localization exponent $\varphi = \pi m S D$ is to use the quasiclassical

expression in Eq.(36). In general, for large $S \gg 1$ the exponent φ is large, the localization cannot be observed, and the above expressions are meaningful only for transport coefficients. Since, according to Eq. (21), the quasiclassical value of S is $S = (2/3\pi)(H/L)^{3/2}$, the quasiclassical estimate of φ (36) is $\varphi \simeq (5/16) \sqrt{\pi/2} (3\pi S/2)^{8/3} (RL/\ell^2) = 24.4S^{8/3} (RL/\ell^2)$. Even for $S = 1$ this is usually a large number (our perturbative equations require $\ell < R, H$), and the localization does not seem feasible. However, for small values of S , the exact quantum expressions for φ are somewhat smaller than their quasiclassical analogs. The best possibility for localization is cooling of the system so that all the particles condense into the lowest miniband ϵ_{0q} (24). Another option is to deal with a system with only one bound or adsorbed state (with a single miniband ϵ_{0q} , Eq.(37)) from the beginning.

The curve $\varphi(\alpha)$ in Figure 1 is plotted for $\beta = R/L = 10$ in the regime $\alpha/\beta^2 = L^2/R\lambda \ll 1$ when the transport coefficients are smooth functions of energy and are not sensitive to step-like changes in the number of accessible minibands S with growing energy (in the figure, S is changing from 1 to 10 with α growing from 0 to 35). In contrast to this, the singularities in transport in the points when the number of accessible minibands changes by 1 manifest themselves acutely at smaller β as in Figure 2 for $\beta = R/L = 0.1$. These singularities are distinct under more or less the same conditions as in our earlier transport calculations for rough films [9,10]. In both Figures φ is too large for weak localization to be observed except for the initial part of the curves which corresponds to small particle energy (small α) when the particles are restricted to the lowest miniband exclusively (24) (see also Figure 3 and Eq.(37)).

FIGURES

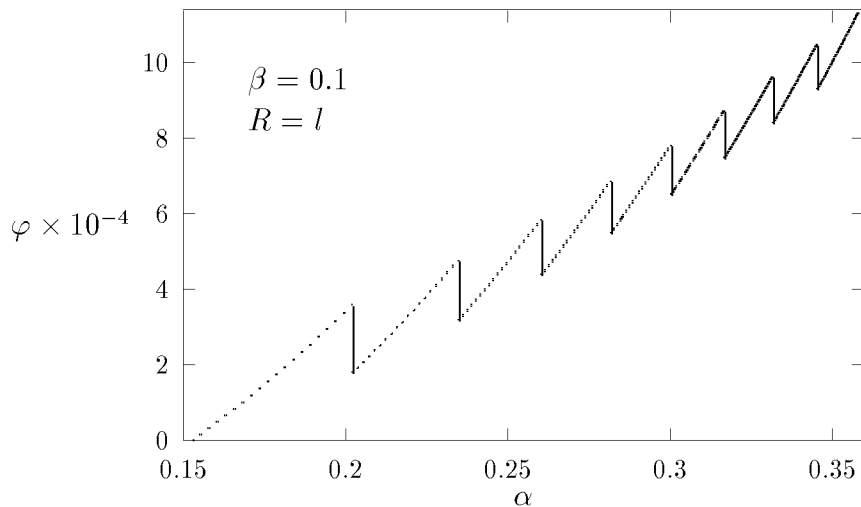


FIG. 1. $\varphi(\alpha, \beta, \ell/R)$, Eq.(22), as a function of $\alpha = R/\lambda$ at $\ell = L$, $\beta = R/L = 10$

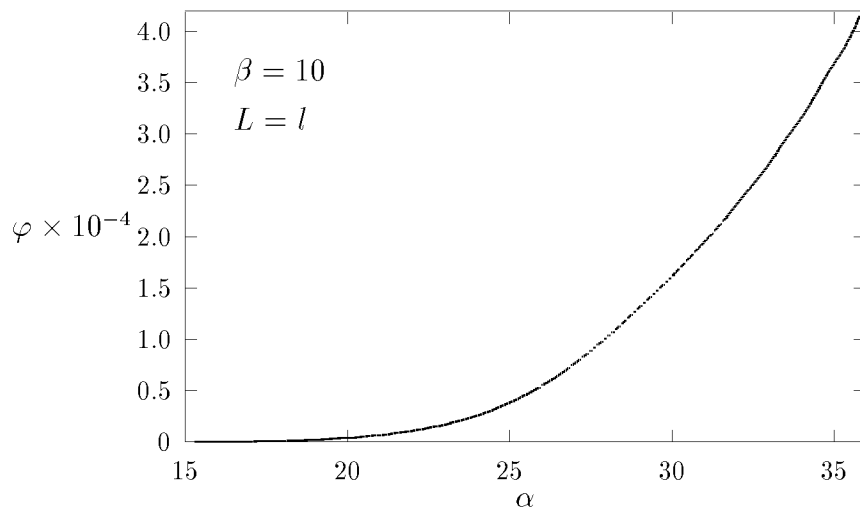


FIG. 2. $\varphi(\alpha, \beta, \ell/R)$, Eq.(22), as a function of $\alpha = R/\lambda$ at $\ell = R$, $\beta = R/L = 0.1$

IV. APPLICATIONS

One of the most interesting applications is the system of ultra-cold neutrons [11] in a gravitational trap with a macroscopically inhomogeneous "floor". For neutrons bouncing in the gravitational field, the main parameters are $L = (2m^2g)^{-1/3} = 5.86 \times 10^{-4} \text{ cm}$, $\alpha = \sqrt{2mER} = 1.6 \times 10^3 Rv$ (here R is measured in cm , and the neutron velocity $v = \sqrt{2E/m}$

- in cm/s). At present, the neutrons can be trapped in a "neutron bottle" with average velocities down to $v = 100 \text{ cm/s}$ ($H \sim 5 \text{ cm}$) [15]. Parameters of the artificially created roughness in experiment [15] were $\ell, R \sim 10^{-2} \text{ cm}$. In typical experiments with trapped ultra-cold neutrons, the distribution of velocities around the average value of v is very narrow and the fraction of low-velocity neutron is insignificant. This means that $H \gg \ell, R \gg L$, and $S \gg 1$, and the above weak localization mechanism cannot be observed in experiments similar to [15] (the localization exponent φ is too large). The localization could become observable only if the neutron energy $E = mv^2/2 = mgH$ is so low that all the neutrons are in the lowest miniband $\epsilon_{0\mathbf{q}}$, Eq.(24). Figure 3 gives the energy dependence of the localization exponent $\varphi(v)$ for this situation in the optimal, from the point of view of weak localization, conditions $\ell = R = L$. As it is clear from Figure 3, the localization can be observed only in a neutron bottle with neutron velocities $v < 2 \text{ cm/s}$ (or $H < 2 \times 10^{-3} \text{ cm}$) and with parameters of inhomogeneities ℓ, R on the scale of L . This also means that the anomalies in neutron count in Ref. [16] with $v \sim 10 \text{ m/s}$, $H \sim 5 \text{ m}$, $S \gg 1$, cannot be explained by the Anderson localization of neutrons since our perturbative calculations are applicable to experimental conditions [16] without modifications. The decrease in number of neutrons coming out of the trap in experiment [16] should be explained by some other process responsible for keeping the neutrons inside the trap.

Instead of further cooling of neutrons, one can try to achieve the localization by using the non-uniform external magnetic field $B(x)$ with the gradient $g\mu\nabla B = 9.6 \times 10^{-20} \text{ erg/cm}$ (B in T) as a holding field instead of gravity mg . The field gradient 1 T/cm is equivalent for neutrons to the gravitational field $g^* = 58g$. This increase in the holding force allows to increase the threshold neutron velocity v by the factor $(g^*/g)^{1/3} \sim 4$. However, this increase in the holding force decreases L and, for the weak localization on the first level to take place, requires scaling down of inhomogeneities.

A similar system with possible localization of particles over an inhomogeneous substrate is the system of electrons above helium or hydrogen surface in the weak electric field. The electron-helium system differs from the trapped ultra-cold neutrons in two ways [17,18].

First, the usual surface inhomogeneities here are ripples and are not static. Though this does not necessarily result in significant changes in the equations, a more straightforward application is the electron system above a thin helium film on the surface of inhomogeneous solid substrate in a setup similar to the quasi-1D electron-helium system of Ref. [19]. The second difference is that the electron in strong electric field creates a dimple on the helium surface. This makes the effective mass dependent on the electric field and leads, in the limit of large fields, to self-trapping or auto-localization of electrons in heavy ripplonic polarons. This dependence of the effective mass on the holding electric field complicates the situation, and the above equations can be used without modifications only in the relatively low electric fields. Numerically, in fields $\mathcal{E} = 10^3 \text{ V/cm}$, mg in Eq.(36) should be replaced by $e\mathcal{E} = 1.6 \times 10^{-9} \text{ erg/cm}$, $L = (2m\epsilon\mathcal{E})^{-1/3} = 1.4 \times 10^{-6} \text{ cm}$, while the scale of inhomogeneities in a realistic setup similar to [19] is rather large, $\ell \sim R \sim 1 \mu\text{m} \gg L$. This means that $S \gg 1$ and one cannot hope to achieve the 2D weak localization without finding a way to scale down the amplitude of inhomogeneities ℓ in this type of experimental setup.

The ripplon localization seems more plausible. For ripples at $T \sim 1 \text{ K}$, the parameters of surface inhomogeneities are $R \sim 20 \text{ \AA}$, $\ell \sim 0.8 \text{ \AA}$ (see below). However, these values of parameters indicate that one has to decrease L in order to observe the localization. This means a considerable increase in the electric field which, in turn, means the creation of dimples. The observation of the weak 2D localization of electrons also requires the decrease in electron velocity down to $v \sim \hbar/mL(\mathcal{E})$. This restriction on kinetic energy corresponds to filling of only the first few minibands. At this point, it is not clear whether this is feasible experimentally.

The best option is, probably, the 2D localization of electrons on the surface of solid hydrogen. Here the experimental challenge is to create the surface roughness of the scale $\ell \lesssim R \sim L = (2m\epsilon\mathcal{E})^{-1/3}$ and cool the electrons to $v \sim \hbar/mL$.

A much more promising system is a system of ultra-cold hydrogen atoms (or molecules) adsorbed on the helium surface or films at temperatures above the 2D condensation. This type of system can be prepared in experiments similar to those developed originally for the

observation of Bose condensation in spin-polarized atomic hydrogen [20,21]. Though the origin of bound states in this system is different from that created by the uniform holding field, the collision probabilities and transport equation still has the form (10), (12). The system has one bound state $\epsilon_0 \sim 1$ K which translates into $L \sim 5$ Å. This size of the bound state is sufficiently large to allow the 2D motion of adsorbed hydrogen particles along the helium surface. This is a purely 2D system with a single miniband $\epsilon_{0\mathbf{q}}$ for which the diffusion coefficient and the localization exponent (24) depend on particle momentum \mathbf{q} as

$$\varphi = \pi m D = \frac{2\gamma L^6}{R^4 \ell^2} \frac{q^2 R^2}{{}_1F_1\left(\frac{3}{2}; 2; -2q^2 R^2\right)} \quad (37)$$

where γ is the insignificant numerical coefficient of the order of unity which is related to the (unknown) derivatives of the particle wave function on the wall $d\Psi(0)/dx$ in Eq.(10). This function $\varphi(q)$ is essentially the same as the function $\varphi(v)$ which is plotted in Figure 3 for neutrons (one should replace v on the horizontal axis by q using $mv^2/2 = \epsilon_0 + q^2/2m$; the most noticeable effect will be the shift of the zero of φ to zero q from the point $v = \sqrt{2m\epsilon_0}$). Here, as for the electrons over helium surface, the main restriction on the direct application of the above equations is that the usual surface perturbations are non-static ripples. Parameters ℓ and R in Eq.(37) play the role of the characteristic amplitude and wavelength of capillary waves $\omega^2 = \sigma k^3/\rho + gk$ with $\sigma/\rho \sim 2.5$ cm³/s². At $T \sim 1$ K, the correlation radius $R \sim 20$ Å, while $\ell \sim 0.8$ Å. Then the coefficient in Eq.(37) is approximately 0.3, and the localization should be observed for particles with momenta q up to $qR \lesssim 1.5$.

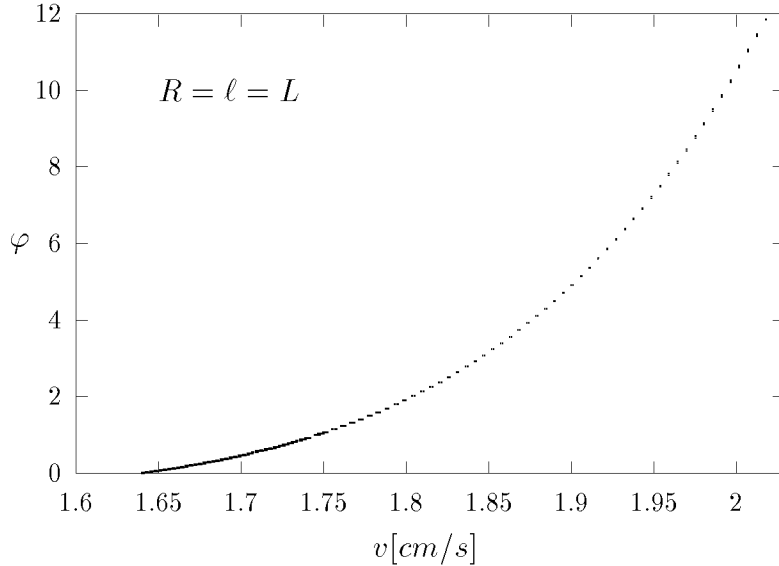


FIG. 3. $\varphi(\alpha, \beta, \ell/R)$, Eq.(22), as a function of (neutron) velocity v at $\ell = L = R$

V. SUMMARY

In summary, we calculated diffusion and localization parameters of a quantum bouncing ball with static random rough wall. The results are expressed explicitly via the energy spectrum of the particle and the correlation function of wall roughness. In three limiting cases the results are analytical and can be applied to any type of the correlation function of surface corrugation and holding potential. Elsewhere, we performed numerical calculations for Gaussian correlations. As possible applications, we discussed ultra-cold neutrons in the gravitational traps, electrons on helium or hydrogen surfaces in electric field, and particles bound to corrugated surfaces with the size of the bound state larger than the corrugation amplitude. In the situations when the experimental observation of weak localization is not feasible, our expressions for the corrugation-driven transport coefficients determine the motion of particles along the wall.

Note that the localization caused by the *dynamic* corrugation, including the ripplon-induced localization, may be different from the above static results in one important aspect. The collision operator (12), (13) contains the matrix element of perturbation in combination

$\langle |V_{jj'}(\mathbf{q}, \mathbf{q}')|^2 \rangle_{\xi} \delta(\epsilon_{j\mathbf{q}} - \epsilon_{j'\mathbf{q}'})$. The simplicity of the collision operator (10) and the transport equation (12), (13) is, to a large extent, the result of the presence of this energy δ -function. In a non-static case, the energy δ -function would have the form $\delta(\epsilon_{j\mathbf{q}} - \epsilon_{j'\mathbf{q}'} - \omega)$. Such a collision operator becomes much more complicated and the *quantum* transport equation - extremely cumbersome [10] when ω is comparable to the wall-defined transition probabilities $W_{jj'}(\mathbf{q}, \mathbf{q}')$. In this resonance frequency range, the quantum bouncing ball problems with static rough wall and dynamic wall are not the same. For the *dynamic* scattering systems in this regime, the wall-defined and bulk-defined transport and localization processes are qualitatively different [10].

VI. ACKNOWLEDGMENT

We are grateful to A. Steyerl for numerous discussions concerning experiments with ultra-cold neutrons. This work was supported by NSF grants DMR-9412769 and DMR-9705304. Some preliminary results were presented at QFS-98 [22].

REFERENCES

- [1] P. A. Lee, and T. V. Ramakrishnan, *Rev.Mod.Phys.*, **57**, 287 (1985)
- [2] B. Altshuler, in: *Nanostructures and Mesoscopic Systems*, eds. W. P. Kirk and M. A. Reed (Academic Press, NY) 1991, p.405-416
- [3] A. McGurn, and A. Maradudin, *Phys.Rev. B* **30**, 3136 (1984)
- [4] P. Arseyev, *JETP Lett.*, **45**, 163 (1987) [*Pis'ma Zh.Eksp.&Teor.Fiz.* **45**, 132 (1987)]
- [5] L. I. Glazman, G. B. Lesovik, D. E. Khmel'nitskii, and R. I. Shekhter, *JETP Lett.*, **48**, 238 (1988) [*Pis'ma Zh.Eksp.&Teor.Fiz.* **48**, 218 (1988)]
- [6] D. A. Wharam *et al*, *J.Phys.C*, **21**, L209 (1988)
- [7] B. J. van Wees *et al*, *Phys.Rev.Lett.*, **60**, 848 (1988)
- [8] V. I. Kozub, and A. A. Krokhin, *J.Phys.: Cond. Matter*, **5**, 9135 (1993)
- [9] A. E. Meyerovich, and S. Stepaniants, *Phys.Rev.Lett.* **73**, 316 (1994); *Phys.Rev. B* **51**, 17116 (1995); *J.Phys.:Cond.Matt.* **9**, 4157 (1997)
- [10] A. E. Meyerovich, and A. Stepaniants, *Phys.Rev. B*, November 1998, in print
- [11] B. Lushchikov, and A. I. Frank, *JETP Lett.* **28**, 607 (1978)
- [12] A. E. Meyerovich, and A. Stepaniants, in: *Condensed Matter Theories*, v. 22 (1998), in print
- [13] J. A. Ogilvy, *Theory of wave scattering from random rough surfaces* (IOP Publishing, Bristol) 1991
- [14] R. M. Feenstra *et al*, *Phys.Rev.Lett.* **72**, 2749 (1994)
- [15] T. Bestle *et al*, *Proc. ISINN-6*, May 1998, to be published
- [16] V. P. Alfimenkov *et al.*, *JETP Lett.*, **55**, 84 (1992) [*Pis'ma Zh.Eksp.&Teor.Fiz.* **55**, 92

(1992)]

- [17] A. J. Dahm, *Low Temp.Phys.* **23**, 639 (1997); I. Karakurt, and A.Dahm, *J. Low Temp.Phys.*, in print (1998)
- [18] S. S. Sokolov, G.-H. Hai, and N. Studart, *Phys.Rev. B* **55**, R3370 (1977)
- [19] Yu. Z. Kovdrya, V. A. Nikolaenko, H. Yayama, A. Tomokiyo, O. I. Kirichek, and I. B. Berkutov, *J.Low Temp.Phys.* **110**, 191 (1998)
- [20] I. Silvera, *J.Low Temp.Phys.* **101**, 49 (1995)
- [21] J. T. M. Walraven, in *Fundamental Systems in Quantum Optics*, eds. J.Dalibard, J.M.Raimond, J.Zinn-Justin, Elsevier, 1992, p.485
- [22] A. Stepaniants, D. Sarkisov, A. Meyerovich, and A. Steyerl, *J. Low Temp.Phys.*, in print (1998)

VII. APPENDIX

We have to calculate the matrix elements $V_{j\mathbf{q},j'\mathbf{q}'}$ of the distortion operator (6),

$$\hat{V} = \frac{\partial U}{\partial X} \xi(\mathbf{s}) - \frac{1}{2m} \hat{P}_x \left[\hat{\mathbf{P}}_s \frac{\partial \xi(\mathbf{s})}{\partial \mathbf{s}} + \frac{\partial \xi(\mathbf{s})}{\partial \mathbf{s}} \hat{\mathbf{P}}_s \right], \quad (38)$$

with the wave functions $\Psi = \Psi_j(X) \exp(i\mathbf{q} \cdot \mathbf{s})$ of the unperturbed Hamiltonian $\hat{H}_0 = \hat{P}^2/2m + U(X)$. The arbitrary potential $U(X)$ contains the infinite barrier at $X = 0$ (*i.e.*, $\Psi_j(0) = 0$), and is either infinite at $X \rightarrow \infty$ ("holding potential") or is attractive with discrete bound states and $U(X \rightarrow \infty) \rightarrow 0$. In both cases, the motion in X direction is finite with $\Psi_j(0) = \Psi_j(\infty) = 0$.

The calculation of the integrals along the wall is trivial and yields $\xi(\mathbf{q} - \mathbf{q}')$ for the first term in (38) and $(q^2 - q'^2) \xi(\mathbf{q} - \mathbf{q}')$ for the second. For the calculation of the integrals over dX ,

$$\int \Psi_j \frac{\partial U}{\partial X} \Psi_{j'} dX = - \int U (\Psi_j' \Psi_{j'} + \Psi_j \Psi_{j'}') dx, \quad (39)$$

we will use the Schrodinger equation for the motion in X direction,

$$\left(\frac{\hat{P}_x^2}{2m} + U\right) \Psi_j = \epsilon_j \Psi_j. \quad (40)$$

Then

$$-\int U (\Psi_j' \Psi_{j'} + \Psi_j \Psi_{j'}') dX = \frac{1}{2m} \int [\Psi_j' \hat{P}_x^2 \Psi_{j'} + \Psi_{j'}' \hat{P}_x^2 \Psi_j] dX - \epsilon_{j'} \int \Psi_j' \Psi_{j'} dX - \epsilon_j \int \Psi_j \Psi_{j'}' dX,$$

and, after integrating by parts, we get

$$\left(\frac{\partial U}{\partial X}\right)_{jj'} = (\epsilon_j - \epsilon_{j'}) \int \Psi_j' \Psi_{j'} dX - \frac{1}{2m} \int \left[\Psi_j' \frac{\partial}{\partial x} \Psi_{j'}' + \Psi_{j'}' \frac{\partial}{\partial x} \Psi_j' \right] dX \quad (41)$$

and

$$\left(\frac{\partial U}{\partial X} \xi(\mathbf{s})\right)_{j\mathbf{q}, j'\mathbf{q}'} = \left[(\epsilon_j - \epsilon_{j'}) \int \Psi_j' \Psi_{j'} dX + \frac{1}{2m} \Psi_j'(0) \Psi_{j'}'(0) \right] \xi(\mathbf{q} - \mathbf{q}') \quad (42)$$

The integral over dX for the second term in (38) is trivial:

$$\left(-\frac{1}{2m} \hat{P}_x \left[\hat{\mathbf{P}}_s \frac{\partial \xi(\mathbf{s})}{\partial \mathbf{s}} + \frac{\partial \xi(\mathbf{s})}{\partial \mathbf{s}} \hat{\mathbf{P}}_s \right]\right)_{j\mathbf{q}, j'\mathbf{q}'} = \frac{1}{2m} \xi(\mathbf{q} - \mathbf{q}') (q^2 - q'^2) \int \Psi_j' \Psi_{j'} dX \quad (43)$$

As a result, the overall matrix element is

$$V_{j\mathbf{q}, j'\mathbf{q}'} = (\epsilon_{j\mathbf{q}} - \epsilon_{j'\mathbf{q}'}) \int \Psi_j' \Psi_{j'} dX + \frac{1}{2m} \Psi_j'(0) \Psi_{j'}'(0), \quad \epsilon_{j\mathbf{q}} = \epsilon_j + \frac{q^2}{2m}. \quad (44)$$

Since we are interested only in the transitional probabilities $W_{jj'}(\mathbf{q}, \mathbf{q}') = \langle |V_{jj'}(\mathbf{q}, \mathbf{q}')|^2 \rangle_\xi$ for the states with $\epsilon_{j\mathbf{q}} = \epsilon_{j'\mathbf{q}'}$, we immediately get Eq.(10):

$$W_{jj'}(\mathbf{q}, \mathbf{q}') \delta(\epsilon_{j\mathbf{q}} - \epsilon_{j'\mathbf{q}'}) = \frac{1}{4m^2} \zeta(\mathbf{q}' - \mathbf{q}) \left| \frac{d\Psi_j(0)}{dX} \right|^2 \left| \frac{d\Psi_{j'}(0)}{dX} \right|^2 \delta(\epsilon_{j\mathbf{q}} - \epsilon_{j'\mathbf{q}'}). \quad (45)$$

This system-independent form of the transition probabilities is not accidental. It is possible to get similar system-independent general expressions for the transition probabilities for many classes of systems with transparent or impenetrable corrugated walls and interfaces including multilayer systems, systems with interwall correlation of inhomogeneities, particles with non-quadratic spectrum, *etc.* [12]

In the case of linear potential $U = mgx$, the derivatives in Eq.(45) can be calculated without using the explicit form of the (Airy) wave functions. Since $\partial U/\partial X = mg$ is a constant, Eq.(41) yields

$$mg\delta_{jj'} = \left[(\epsilon_j - \epsilon_{j'}) \int \Psi_j' \Psi_{j'} dX + \frac{1}{2m} \Psi_j'(0) \Psi_{j'}'(0) \right]$$

or, for $j = j'$, $mg = [\Psi_j'(0)]^2/2m$. Then the transition probability (45) obtains the form (11),

$$W_{jj'}(\mathbf{q}, \mathbf{q}') \delta(\epsilon_{j\mathbf{q}} - \epsilon_{j'\mathbf{q}'}) = m^2 g^2 \zeta(\mathbf{q}' - \mathbf{q}) \delta(\epsilon_{j\mathbf{q}} - \epsilon_{j'\mathbf{q}'}). \quad (46)$$

VIII. FIGURE CAPTIONS

Figure 1. $\varphi(\alpha, \beta, \ell/R)$, Eq.(22), as a function of $\alpha = R/\lambda$ at $\ell = L$, $\beta = R/L = 10$.

Figure 2. $\varphi(\alpha, \beta, \ell/R)$, Eq.(22), as a function of $\alpha = R/\lambda$ at $\ell = R$, $\beta = R/L = 0.1$

Figure 3. $\varphi(\alpha, \beta, \ell/R)$, Eq.(22), as a function of (neutron) velocity v at $\ell = L = R$